Christian Pluchar
Mentor: Keita Kawabe
LIGO SURF 2017 Second Interim Report
Measuring Scattered Light Off LIGO Test Masses

Introduction

The Advanced LIGO detectors are four kilometer long Michelson interferometers. Improvements to the detectors in past years have resulted in multiple detections of gravitational waves from binary black hole mergers. Additional improvements to lower noise from terrestrial and detector sources and progress towards the Advanced LIGO design sensitivity will allow for a larger signal to noise ratio in the detector. The interferometer measures the change in distance between two test masses relative to each other. Through a series of additional optical features designed to increase the effective beam length, kilowatts of laser power are present in the beam cavities during observation, and despite the precision of the mirrored surface of each of the test masses, some light scatters off the test masses and out of the beam path [1]. DSLR cameras have been installed at the LIGO Hanford Observatory which can be used to observe this scattering. Detector sensitivity increases as the power circulating in the beam cavity increases [1], so minimizing scattering off of the test masses will lead to better performance. In order to measure the amount of energy scattered off the test masses, the cameras must be calibrated to equate the sensor output to the corresponding energy which was incident on the sensor.

Methods

Camera Calibration and Measuring Power Scattered Off Test Masses

Cameras sensors contain semiconductors which absorb light and produce current. In the CMOS sensor of the Nikon D7100 and D810 cameras being used, each pixel site has its own amplifier, and the current is turned into a corresponding digital number based on the specifics of the camera and its settings. Digital cameras utilize three separate types of photosensors - one type is sensitive to green light, one type is sensitive to red light, and the final is sensitive to blue light. They are arranged in a pattern known as a bayer filter and used to create color images with a similar color palette as the human eye [2]. These sensors have limited sensitivity in other wavelengths as well, including the infrared range. The main lasers of the LIGO detectors have a wavelength of 1064 nanometers [3], which the camera sensor still is sensitive to, despite it being in the infrared range. In order to increase the response to this wavelength of light, the IR filter installed in the camera was removed. Calibration was first performed with an attenuated 980 nanometer laser to refine the data collection and analysis process, and then with a 1064 nanometer laser to match the wavelength used in the detector.

The purpose of the camera calibration is to calculate a conversion from the digital output of the camera sensor into a quantity of light energy incident on the sensor. The camera lens was

removed and the camera was placed on a tripod. A laser was installed on an adjacent optical table and directed so that the beam was directed on the sensor of the camera. A laser power meter was used to measure the power produced by the laser. The lights of the room were turned off, and exposures were taken using different shutter speeds, laser powers, and laser beam profiles. Care was taken in order to ensure the entire beam was directed on the sensor and that a minimum numbers of pixels were overexposed (saturated). The camera has a maximum value for each pixel value, and reaching this value prohibits the camera from sensing additional light incident at that photosite. A series of photos were also taken with the laser turned off in order to measure the ambient light in the room and the dark offset of the camera pixels. The ISO of the camera was kept constant at 200, and the image color depth was set to 14 bits. A Python script using Rawpy was then utilized to measure the digital output of the camera from the RAW files produced.
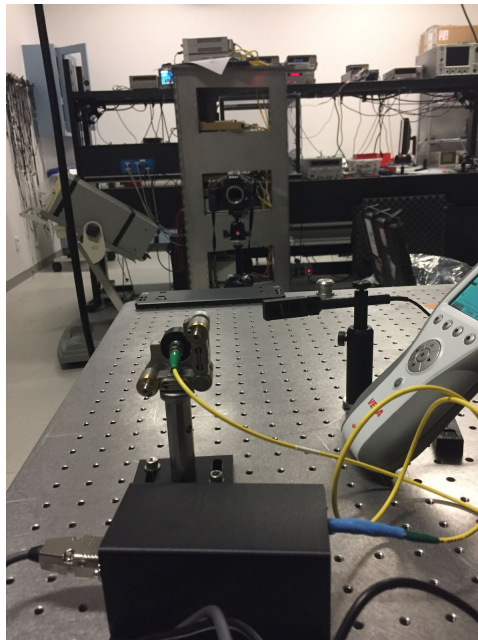

Figure 1: Experimental setup for camera calibration. A laser (foreground) was directed at the camera sensor and images were captured at different power levels of the laser and shutter speeds of the camera. A laser power meter (right) was used to measure the power of the laser.

Digital single-lens reflex (DSLR) cameras have been previously installed at viewports across the detector. At the end stations, these have been added in order to observe the beam positioning of the photon calibrator on the test masses [4]. Because these viewports are offset from the test masses by a considerable distance, zoom lenses have been installed in order to capture finer detail. The cameras are controlled by remote capture software. The camera at ETMx was used to capture images of the scattering, both while the interferometer was in lock and while it was out of lock in order to measure the scattered light from other sources that are not

the main laser. Previously captured images of ITMx will be used as well in analysis, and a similar method was used to capture them. Using the calibration information of the camera and these images, an estimate of the amount of power from the main laser off the test masses can be made.

Photon Absorption

An important metric of camera sensor performance is the percentage of photons incident on the sensor that are absorbed by the sensor, commonly referred to as quantum efficiency [5]. Large areas of the sensors, particularly CMOS sensors like the ones used in our measurement, have area covered by components, such as amplifiers, which are not photosensitive and used to measure light incident on the sensor. Additionally, the photosensitive components do not absorb all the light that is incident on them. The amount of light absorbed by each is dependent on the composition of the type of detector (red, green or blue in the case of the sensors used) and the frequency of light incident.

In order to determine the quantum efficiency of the sensor, a large number of exposures were taken in succession with laser light incident on the sensor with the lights in the room turned off. The camera settings and power setting of the laser were kept constant during the exposures. A remote shutter trigger was used as to not move the camera. The length of the shutter speed was chosen to be significantly slower than the flash sync speed of the camera.

A Python script was then used to find the mean and standard deviation of the number of counts at each pixel for each of the exposures with the laser incident on the sensor. The primary effect trying to be observed is the shot noise of the light source. The photons emitted by the laser are discrete units, and similarly, they arrive at the camera sensor as discrete units as well. There are fluctuations on the number of photons that arrive at the sensor per unit time due to the discrete nature of light. The distribution formed by the difference in photon arrivals is a Poisson distribution, and therefore, for a mean of N photons arriving at the sensor, the standard deviation of photons arriving at the sensor is $\sqrt{N}$. There are other effects to consider as well, including variations in the power output of the laser not due to shot noise, and the electronic noise of the camera as well. The amplitude noise of the laser comes from physical parameters in the laser, such as the temperature, varying as it operates, therefore changing its output. Its contribution to the standard deviation is linearly proportional to the number of photons incident. The electronic noise originates from the amplifiers on the camera sensor, and is a constant effect for a chosen camera setting. Taking into account all of these effects, our model for the standard deviation as a function of mean camera counts for a pixel is:

$$StDev = sqrt(a + b*(N) + c*(N)^2), (Eq. 1)$$

where N is the number of photons incident, a is the electronics noise term, b is the shot noise coefficient, and c is the amplitude noise coefficient. If all the photons are absorbed, the value of b will be one. Lower values of b indicate not all incident photons are absorbed by the sensor.

Results

One of the first important questions to address with the camera calibration was to determine if the calibration was independent of beam profile.
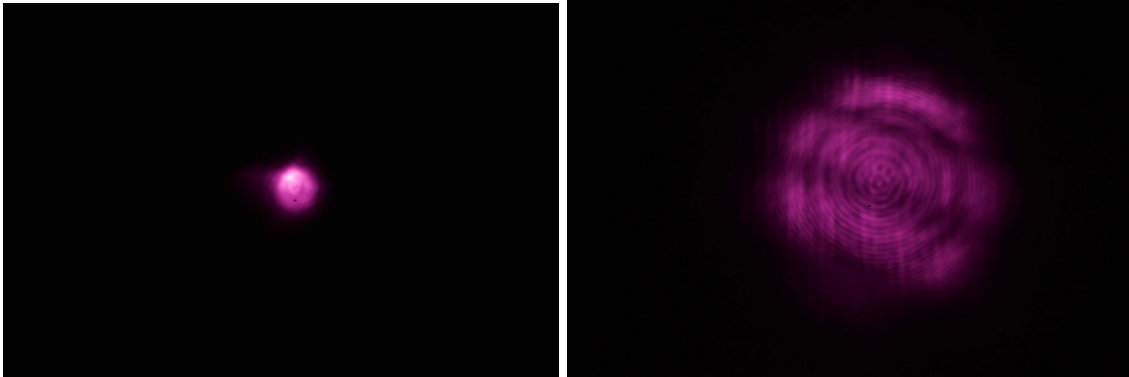

Figure 2: Sample images showing the narrow (left) and wide (right) beam profiles used in the 980nm calibration.

Previous results [6] showed that the calibration could be dependent on beam profile. Because the individual sensors have a linear response between the number of electrons produced and the number of photons incident for a particular wavelength of light, the distribution of light across the sensor should not matter for the digital output (ignoring cases of saturation). This result is inconsistent with how the camera works. The result also poses additional complications for the ultimate experimental goal as the scattering off the test mass will have a different beam profile than the laser used for the calibration.

To address this question, in each set of data a series of exposures were taken with two sets of beam profiles. In every set of data collected, the differences between the calibrations of the different beams profiles were found to be small and within the combined error of the power measurement of the laser and statistical error.
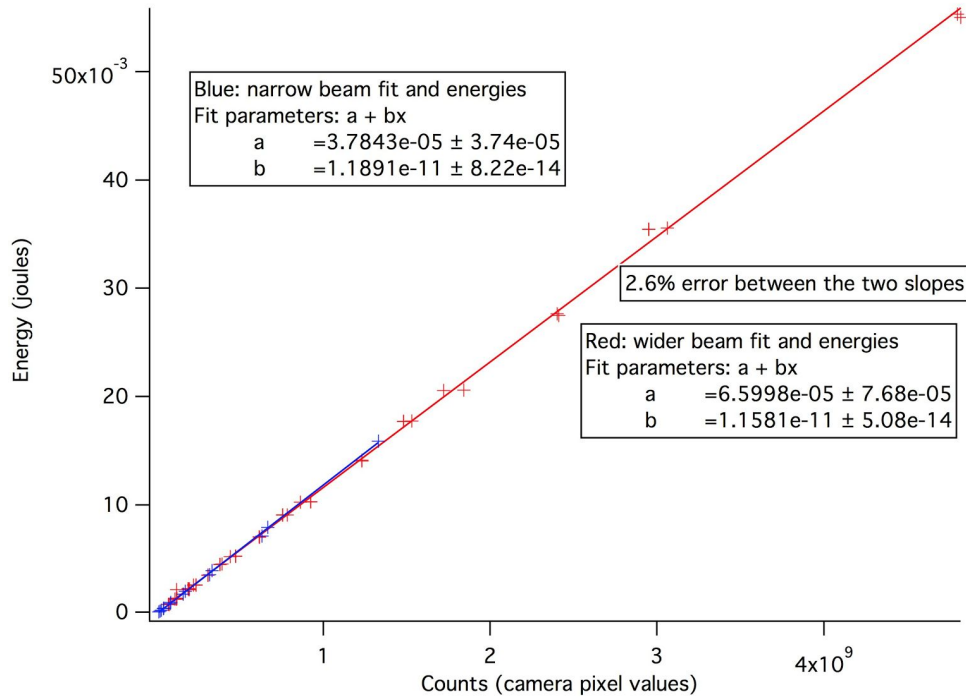
Figure 3: Beam profile comparison for the 980nm laser. The slopes of the lines represent the conversions between the sensor output (counts) and the energy incident on the sensor.
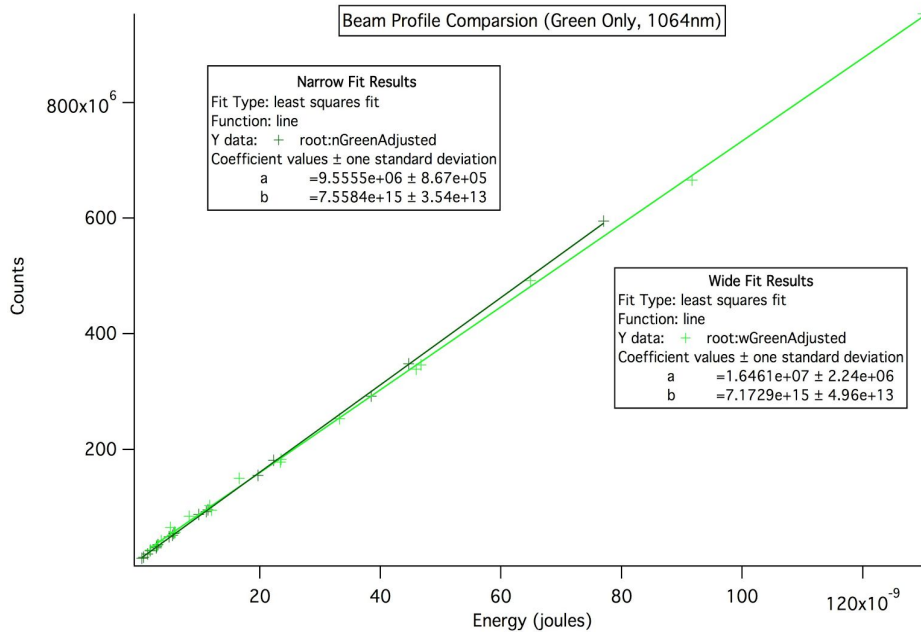

Figure 4: Beam profile comparison for 1064nm laser. Only the green channel has been shown here. There is roughly a 5% difference between the two slopes.

Re-examining the 2016 data, the calibration for the wide beam profile is roughly consistent with the data that I took (to about a factor of two, which can be attributed to the difference in ISO used in the calibration. The difference in the other beam profile data cannot be explained exactly, however, it is possible for it to be due to a measurement error in the laser power.
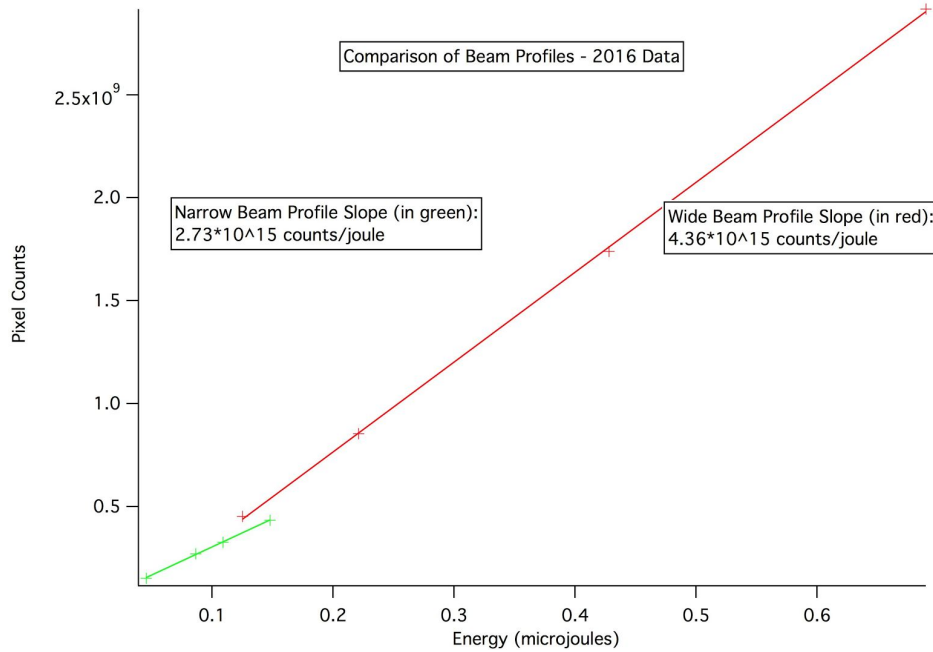

Figure 5: Beam profile comparison of 2016 data. Note the very different slopes for the two different beam profiles tested.
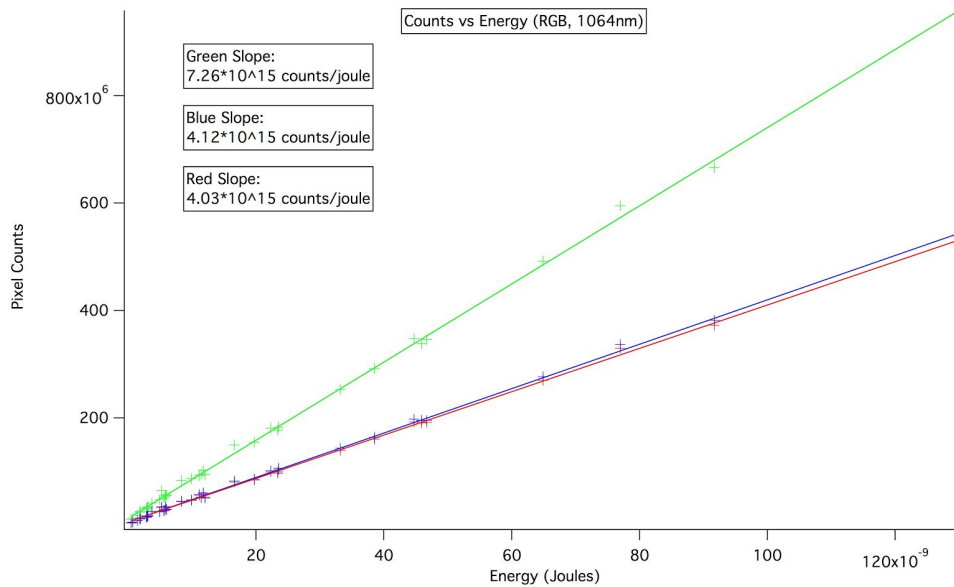

Figure 6: Calibration for all three color channels, D7100. Both sets of beam profile data are used.

Color	Slope (Counts/Joule)	Standard Deviation
Red	1.61*10^16	9.32*10^13
Green	1.45E*10^16	8.26*10^13
Blue	1.65E*10^16	9.52*10^13

Table 1: Nikon D7100 1064nm Calibration Results. A linear fit was performed on all of the data collected with the 1064nm laser, and the calibration (in counts/joule) were found for the red, green, and blue channels. The camera was set to ISO 200 and 14 bits were used to record the values on each channel. Note that these slopes are different than the output of the fits of the graphs. These results have been adjusted to account for the fact that not all of the energy incident on the sensor falls on each color sensor equally (half of the energy falls on the green sensors, a quarter falls on both blue and red) because of the Bayer filter arrangement.

The calibration was first performed with a Nikon D7100 camera. A second camera, a Nikon D810, was calibrated using an identical procedure. These two models of cameras have both been used to make observations on the test masses.
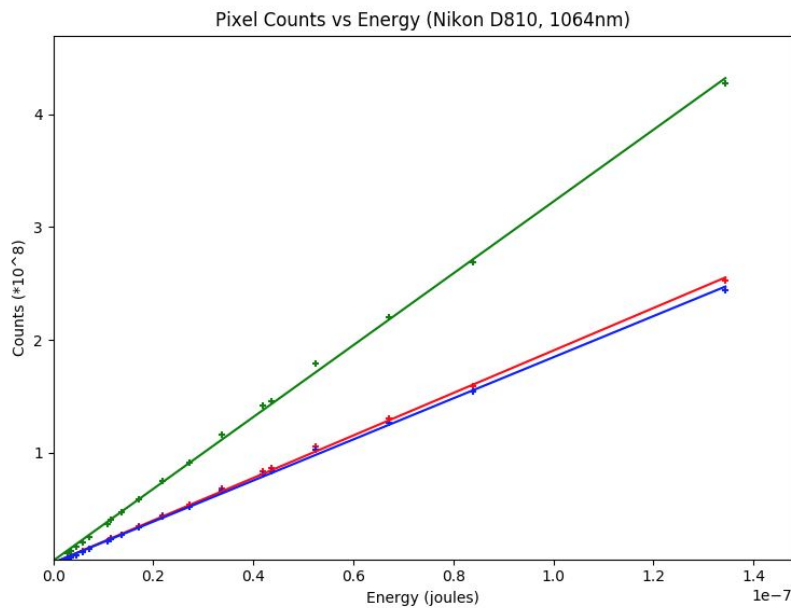

Figure 7: Pixel Counts vs Energy for the Nikon D810. An identical calibration procedure was performed for the D810 as the D7100.

Color	Slope (Counts/Joule)	Standard Deviation
Red	7.53*10^15	1.33*10^13
Green	6.37*10^15	2.36*10^13
Blue	7.28*10^15	1.30*10^13

Table 2: Nikon D810 1064nm Calibration Results. Adjustments have been made to account for the relative area of each of the specific color sensors on the sensor.

A D7100 camera mounted in one of the viewports using a facing the end test mass in the X-arm (ETMx) used for the photon calibration system was used to measure the amount of power being scattered off the mirror. A number of different exposures at different shutter speeds were recorded while the interferometer was locked. The camera calibration for the D7100 was used to calculate the power of the light being scattered off the test mass. From the viewport position, the power scattered off the test mass was 7.3 +/- .6 * 10^-6 watts. The transmissivity of the viewport has not been included in this calculation. It should be also noted that the scattering off the test mass is almost certainly not uniform, and this measurement made using observations at one angle from the mirror.
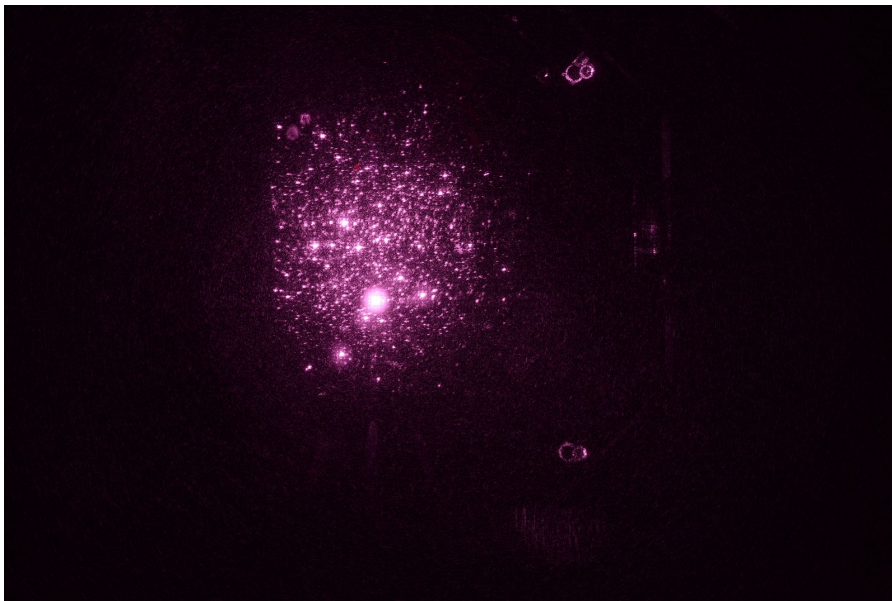

Figure 8: Sample of photo of the ETMx scattering. Note the saturated pixels, and the red laser light being recorded by the camera as well near the top of the image. The following photo was taken using ⅛ shutter time and at ISO 100, but even at faster shutter speed, many pixels still saturated.

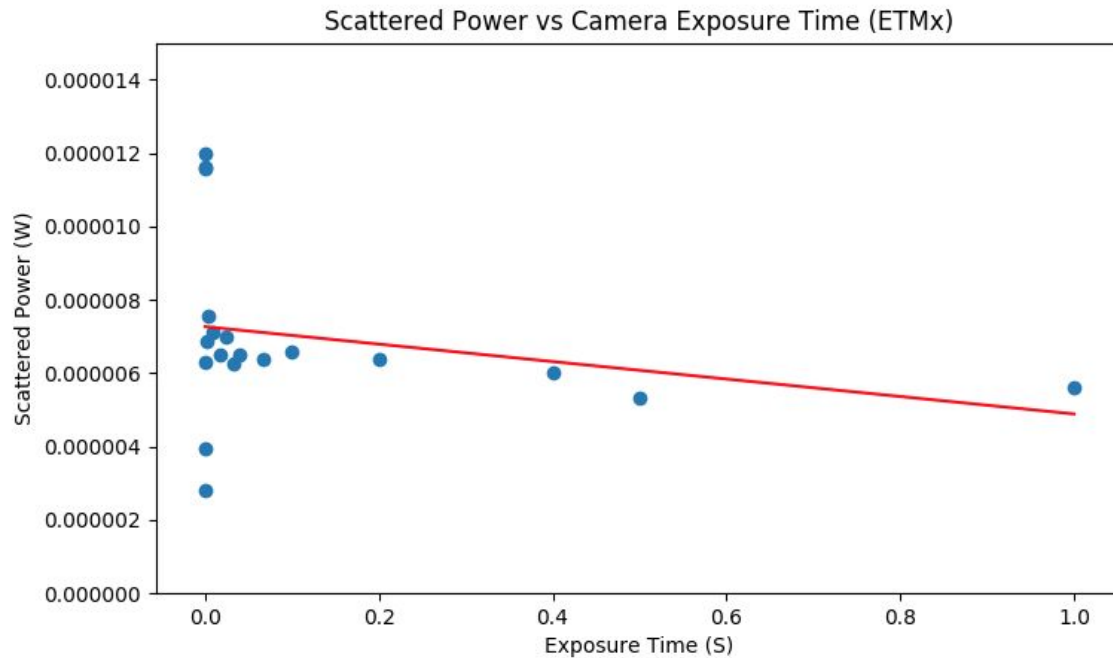*Figure 9: Scattered power versus the exposure time of ETMx captured with a Nikon D7100 camera used for Pcal. The slope of the fitted line is -2.38 * 10^-6 +/- 2.20*10^-6. This does not quite agree with zero, which would indicate a constant power measured regardless of exposure time used to measure the power. The negative slope is consistent with the fact that at slower shutter speeds, more of the image was saturating. The power was calculated using the Y-intercept of the fitted line. Further investigation into why the spread of the measurements taken with fast shutter speeds is very large is needed.*

Photon Absorption

       Efforts to measure the percentage of photons absorbed by the sensor have encountered a number of challenges. For starters, due to the number of images and the size of images used in the analysis, the calculations have exhausted the memory limits of my personal computer. In an attempt to get around these limitations, two ideas have been implemented. The first was to sum up a 10x10 grid of pixels in each image and treat that as a single pixel. This reduces the final number of data points by a factor of 100 and greatly reduces the computational resources needed. Additionally, in the analysis, groups of images have been grouped together and analyzed separately and then combined together later instead of analyzed all at once, reducing the peak memory used.

       The main problem encountered is a "drift" of the light incident on the sensor. While combining adjacently captured images tends to reduce the standard deviation, combining images

that were taken apart from each other largely increases the standard deviation around some mean pixel counts. Inspecting the images, there is subtle difference in the interference pattern of the laser beam on the image sensor between images taken apart in time.

In an attempt mitigate this effect, the light source was switched from a laser to a green LED. While it was possible to use a larger number of images without dramatically increasing the standard deviation in some regions, attempting to use the entire data set resulted in the same effect as the laser light source. The apparent variation of the beam on the sensor as a function of time needs further investigation. Additionally, the green light of the LED is only being detected by the green photosites on the camera sensor (which is to be expected). Using the LED for this measurement therefore gives us no information about the absorption rate of the red or blue channels. Additionally, even though the green photosites absorb the infrared wavelengths used in the main laser as well as the green LED laser, they may not absorb them at the same rate.
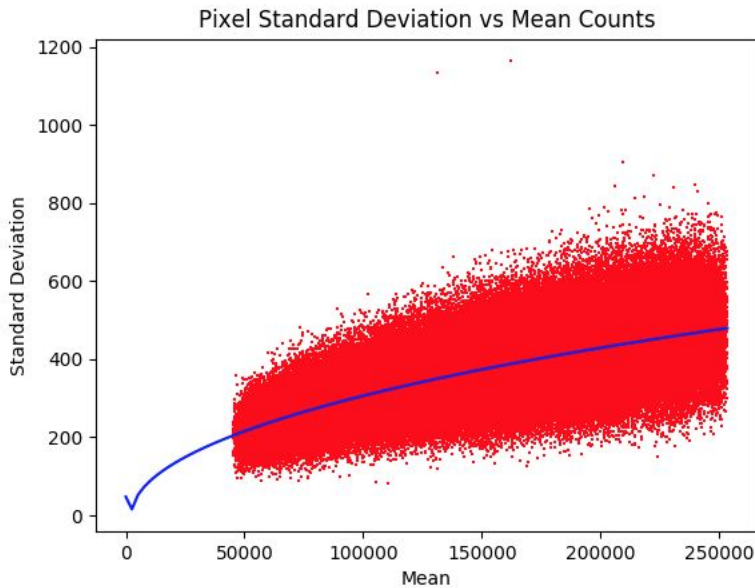

Figure 10: The standard deviation of pixel sites versus the mean of the pixel site across 15 images for the LED light source.
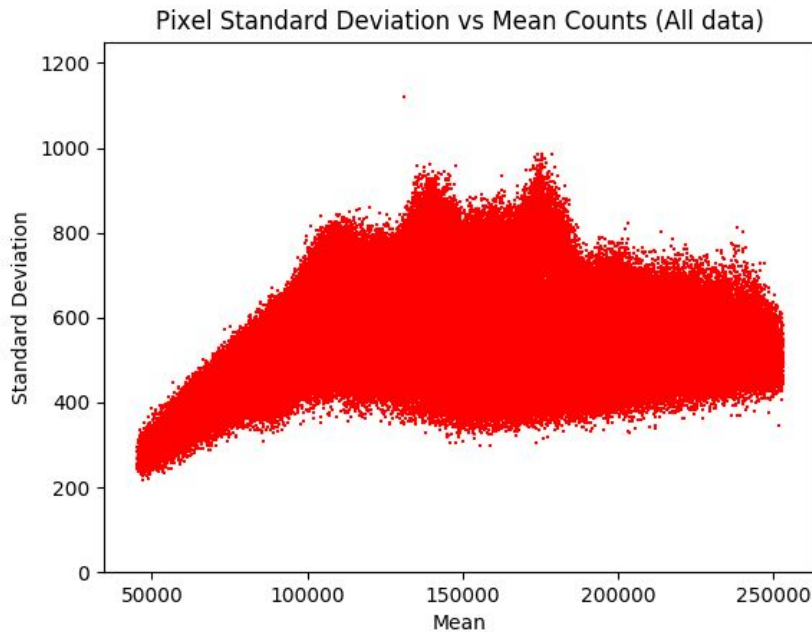
Figure 11: The standard deviation of pixel sites versus the mean of the pixel site across 90 images for the LED light source. Some regions the spread of the standard deviations decreases with more images being added, as expected, which helps attain a fit with a smaller statistical error. Other places it increases, such as in the center. Our model does not describe this distribution of points.

Further Work

       In my remaining time, I hope to continue to analyze the amount of power scattering off the test masses. Previously captured images of ITMx can be analyzed as well. Measurements on other test masses or further refinements in the analysis could be pursued. Using my camera calibration, the position of the camera, and transmissivity of the lens used, I plan to calculate an estimate for the total amount of power scattered by the test masses. Additionally, I hope to resolve issues in my experiment to measure the quantum efficiency of the camera sensor.

References

1. B. P. Abbott, et al., GW150914: The Advanced LIGO detectors in the era of first discoveries, Physical Review Letters, 116, 131103 (2016).
2. Digital Camera Sensors, WWW Document, (http://www.cambridgeincolour.com/tutorials/camera-sensors.htm).
3. LIGO's Laser, WWW Document, (https://www.ligo.caltech.edu/page/laser).
4. S. Karki, et al., The Advanced LIGO Photon Calibrators, https://arxiv.org/pdf/1608.05055.pdf (2016).

5. Quantum Efficiency, WWW Document, (https://www.rp-photonics.com/quantum_efficiency.html).
6. Chen Jie Xin, Development of optical imaging system for LIGO test mass contamination and beam position monitoring, LIGO Document Control Center, (https://dcc.ligo.org/DocDB/0128/T1600390/002/ligo_final_report.pdf).